

# Synthesis, X-ray Geometry, and Anodic Behavior of Tris[2-(hydroxymethyl)phenyl]phosphane

Florence Chalier,<sup>†</sup> Yves Berchadsky,<sup>†</sup> Jean-Pierre Finet,<sup>†</sup> Gérard Gronchi,<sup>‡</sup> Sylvain Marque,<sup>†</sup> and Paul Tordo<sup>\*,†</sup>

Laboratoire de Structure et Réactivité des Espèces Paramagnétiques, Case 521, Unité de Recherche Associée n° 1412 au Centre National de la Recherche Scientifique, Université de Provence, Avenue Escadrille Normandie-Niemen, 13397 Marseille Cedex 20, France, and Laboratoire d'Electrochimie de l'ENSSPICAM, Unité de Recherche Associée n° 1410 au Centre National de la Recherche Scientifique, Université d'Aix-Marseille III, Avenue Escadrille Normandie-Niemen, 13397 Marseille Cedex 20, France

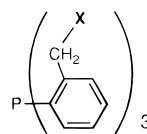
Received: September 25, 1995<sup>Ⓞ</sup>

Tris[(monohydroxymethyl)phenyl]phosphanes **5a** and **5b** were prepared, and the geometry of the *ortho*-isomer **5a** was determined by X-ray diffraction. **5a** was found to be propeller-like in shape, exhibiting a helical conformation with the three hydroxymethyl substituents standing on the same side as that with the phosphorus lone pair. Phosphanes **5a** and **5b** underwent electrochemical one-electron oxidation, giving rise to nonpersistent phosphoniumyl cation radicals **5a**<sup>+</sup> and **5b**<sup>+</sup>. The low value of the anodic peak potential of **5a** was explained by the fast decay of **5a**<sup>+</sup>, which was rapidly rearranged to a phosphoranyl radical through the formation of a strong P–O bond. The fast oxidation of this intermediate phosphoranyl radical followed by a second cyclization led to the 1-[2-(hydroxymethyl)phenyl]spirobi[1*H*,3*H*-2,1-benzoxaphosphole] **7a**, which was isolated in significant yield.

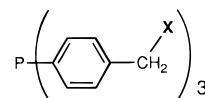
## Introduction

The persistence of phosphoniumyl cation radicals, derived from triarylphosphanes, is largely dependent on the steric hindrance of the aryl groups.<sup>1,2</sup> Electronic effects of the substituents on the radical cation half-lives have been studied essentially in the case of through-bond inductive effects<sup>1,2</sup> and electron delocalization into aromatic rings.<sup>1,3</sup> X-ray studies and force field calculations have shown that 2,6-disubstitution on at least two of the three aryl ligands leads to a significant flattening of the pyramidal structure of the molecule.<sup>2,4</sup> Then a greater contribution of the phosphorus 3p orbital in the HOMO<sup>2,5</sup> results in an increase of its energy level and thus in a greater oxidizability of triarylphosphanes substituted with methyl substituents or electron-withdrawing substituents like the chlorine atom.<sup>1,2</sup> On the other hand, in the absence of oxygen, crowding of the radical center makes the corresponding phosphoniumyl cation radicals significantly persistent. However, methoxy *ortho*- and *para*-substituted phosphanes present a very low oxidation peak potential as well as a completely irreversible oxidation due to the rapid evolution of the radical cations through intramolecular processes. McEwen *et al.* pointed out the faster quaternization reaction rate of triarylphosphanes substituted in the *ortho* position by methoxy or dimethylamino groups compared to their *para* analogues.<sup>6,7</sup> This result was attributed to an interaction between the 2p electrons of a heteroatom and the incipient positive P<sup>IV</sup> center in the early transition state. Similarly, according to the X-ray crystal structure of tris[2-(dimethylaminomethyl)phenyl]phosphane,<sup>8</sup> intramolecular coordination of the phosphorus P<sup>III</sup> atom was suggested. Furthermore, a through-space heteroatom–phosphorus P<sup>III</sup> atom interaction in tris[2-(trifluoromethyl)phenyl]phosphane resulted in an enhanced electronic density on the phosphorus atom, leading to an easy electron removal by vertical ionization.<sup>9</sup>

## SCHEME 1



X = OH, OMe, NMe<sub>2</sub>, SMe



X = OH, OMe, NMe<sub>2</sub>, SMe

In our investigation of the factors influencing the life span and the structure of triarylphosphoniumyl radicals, we have studied the anodic behavior of a series of heterosubstituted triarylphosphanes shown in Scheme 1. In this paper, we will report on the synthesis, structural studies and electrochemical investigations of two new phosphanes, the tris[2- or 4-(hydroxymethyl)phenyl]phosphanes **5a** and **5b**.

## Experimental Section

**Chemicals.** All reactions were carried out under a dry, oxygen-free nitrogen atmosphere. The glassware was dried in an oven at 120 °C and flushed with nitrogen after assembling. Solvents were dried by distillation on sodium/benzophenone for THF and on magnesium for methanol. All solvents for syntheses, crystallization, and analyses were deoxygenated, and the samples were stored under nitrogen. Melting points were taken on a Büchi capillary apparatus and have been left uncorrected. NMR spectra were obtained on Varian EM 360 A (<sup>1</sup>H NMR 60 MHz), Bruker AC 100 (<sup>31</sup>P NMR 40.5 MHz), and Bruker AM 400 X (<sup>1</sup>H NMR 400 MHz and <sup>13</sup>C NMR 100.6 MHz) spectrometers. Unless otherwise stated, chemical shifts are reported as δ values relative to internal and external tetramethylsilane for <sup>1</sup>H and <sup>13</sup>C NMR, respectively, and to external 85 wt % phosphoric acid for <sup>31</sup>P NMR. Mass spectra were performed on a Varian MAT 311 spectrometer.

Compounds **2a**, **3a** [<sup>31</sup>P NMR (CDCl<sub>3</sub>) δ –35.9], and **4a** [<sup>31</sup>P NMR (CDCl<sub>3</sub>) δ –21.9] were prepared using the Schiemenz and Kaack procedure.<sup>10</sup>

*Tris[2-(hydroxymethyl)phenyl]phosphane 5a.* (a) *Reduction of 4a.* A mixture of sodium borohydride (0.58 g, 15.3 mmol)

\* To whom all correspondence should be addressed.

<sup>†</sup>Université de Provence.

<sup>‡</sup>Université d'Aix-Marseille III.

<sup>Ⓞ</sup> Abstract published in *Advance ACS Abstracts*, December 15, 1995.

and tris(2-formylphenyl)phosphane **4a** (2 g, 5.8 mmol) in dry methanol (100 cm<sup>3</sup>) was stirred at room temperature for 30 min. The solution was concentrated, and water was added. The white precipitate was filtered and dried. After recrystallization from CH<sub>2</sub>Cl<sub>2</sub>–ethyl alcohol (95:5), tris[2-(hydroxymethyl)phenyl]phosphane **5a** was obtained as cream-colored crystals (1.3 g, 65% yield), mp 193–195 °C. <sup>31</sup>P NMR: δ (DMSO), –35.2; δ (CD<sub>3</sub>OD) –35.5. <sup>1</sup>H NMR (DMSO, 400.13 MHz) δ: 7.619 (3H, ddd, *J*<sub>H<sub>3</sub>P</sub> = 4.5 Hz, *J*<sub>H<sub>3</sub>H<sub>5</sub></sub> = 1.0 Hz, *J*<sub>H<sub>3</sub>H<sub>4</sub></sub> = 7.5 Hz, H-3), 7.416 (3H, dt, *J*<sub>H<sub>4</sub>H<sub>3</sub></sub> = *J*<sub>H<sub>4</sub>H<sub>5</sub></sub> = 7.5 Hz, *J*<sub>H<sub>4</sub>H<sub>6</sub></sub> = 1.3 Hz, H-4), 7.184 (3H, dt, *J*<sub>H<sub>5</sub>H<sub>4</sub></sub> = *J*<sub>H<sub>5</sub>H<sub>6</sub></sub> = 7.5 Hz, *J*<sub>H<sub>5</sub>H<sub>3</sub></sub> = 1.0 Hz, H-5), 6.626 (3H, ddd, *J*<sub>H<sub>6</sub>–P</sub> = 4.9 Hz, *J*<sub>H<sub>6</sub>H<sub>5</sub></sub> = 7.5 Hz, *J*<sub>H<sub>6</sub>H<sub>4</sub></sub> = 1.3 Hz, H-6), 5.274 (3H, t, *J* = 4.6 Hz, OH), and 4.548 (6H, dd, *J*<sub>H–P</sub> = 1.5 Hz, *J*<sub>H–OH</sub> = 4.6 Hz, CH<sub>2</sub>). <sup>13</sup>C NMR (DMSO, 100.6 MHz) δ: 60.87 (CH<sub>2</sub>, *J*<sub>CP</sub> = 28.17 Hz), 126.27 (C-3, *J*<sub>CH</sub> = 49.79 Hz, *J*<sub>CP</sub> = 5.03 Hz), 129.10 (C-4, *J*<sub>CH</sub> = 39.74), 131.43 (C-1, *J*<sub>CP</sub> = 12.07 Hz), 132.38 (C-6, *J*<sub>CH</sub> = 49.79 Hz), and 149.29 (C-2, *J*<sub>CP</sub> = 32.43 Hz). High resolution MS (HRMS) found, 352.1235; C<sub>21</sub>H<sub>21</sub>O<sub>3</sub>P requires 352.1228; *m/e* (70 eV), 352 (6.6%, M<sup>+</sup>), 349 (3.5), 321 (21.3, M<sup>+</sup> – CH<sub>2</sub>–OH), 316 (28.1), 303 (64.3), 297 (13), 243 (22.1), 213 (12.5), 196 (16.5), 178 (100), 165 (56.9), 152 (15.9), 137 (19.2), 119 (11.7), 109 (13.9), 107 (23.1, C<sub>6</sub>H<sub>4</sub>CH<sub>2</sub>OH<sup>+</sup>), 91 (99.3), 89 (16.6), 77 (43.9), 65 (20.4), 63 (11.3), 51 (29.4), 47 (15.5), 39 (19.1), and 31 (23.4, CH<sub>2</sub>OH<sup>+</sup>).

(b) *Synthesis from 2-Bromobenzyl Alcohol.* A solution of *n*-butyllithium (2.5 M in hexane, 21.4 cm<sup>3</sup>, 53.4 mmol) was added dropwise over 30 min into a cooled (–25 °C) solution of 2-bromobenzyl alcohol (5 g, 0.0267 mol) in dry THF (50 cm<sup>3</sup>) with the temperature maintained below –20 °C. The mixture was stirred for 2 h at –20 °C. Then phosphorus trichloride (0.70 cm<sup>3</sup>, 8.02 mmol) was added slowly at –25 °C and the mixture was stirred for 2 h at –20 °C. After addition of a 5% sodium hydrogen carbonate aqueous solution (20 cm<sup>3</sup>), THF was distilled under vacuum and the solid was filtered from the aqueous phase. A white solid (0.96 g) of oxidized products was removed from the mixture by crystallization in CH<sub>2</sub>Cl<sub>2</sub>, and the tris[2-(hydroxymethyl)phenyl]phosphane **5a** (1.035 g, 37% yield) was crystallized from the oily yellow residue by treatment with CH<sub>2</sub>Cl<sub>2</sub>–ethyl alcohol (95:5).

*Tris[4-(1,3-dioxacyclopent-2-yl)phenyl]phosphane 3b.* The Grignard reagent prepared from 2-(4-bromophenyl)-1,3-dioxolane<sup>11</sup> (12.82 g, 0.0559 mol) and magnesium fine powder (1.36 g, 0.0559 mol) in dry THF (50 cm<sup>3</sup>) under sonication was cooled at 0 °C, and a solution of phosphorus trichloride (1.22 cm<sup>3</sup>, 0.014 mol) in THF (4 cm<sup>3</sup>) was then slowly added. The mixture was stirred for 12 h at room temperature and then was refluxed for 3 h. After cooling at 0 °C, a saturated aqueous solution of sodium hydrogen carbonate (10 cm<sup>3</sup>) was added. The mixture was extracted with CH<sub>2</sub>Cl<sub>2</sub> (100 cm<sup>3</sup>). The organic phase was washed with water, dried on MgSO<sub>4</sub>, and concentrated under reduced pressure. Crystallization from THF–ethanol (4:1) at 4 °C gave the title compound **3b** as white crystals (3.5 g, 45% yield), mp 149 °C. Found: C, 67.79; H, 5.72. C<sub>27</sub>H<sub>27</sub>O<sub>6</sub>P requires C, 67.78 and H, 5.69%. <sup>1</sup>H NMR (CDCl<sub>3</sub>, 60 MHz) δ: 7.9–7.1 (12H, m, ArH), 5.8 (3H, s, ArCH), and 4.4–3.9 (12H, m, OCH<sub>2</sub>–CH<sub>2</sub>O). <sup>31</sup>P NMR (CDCl<sub>3</sub>) δ: –7.1.

*Tris(4-formylphenyl)phosphane 4b.* A mixture of tris[4-(1,3-dioxacyclopent-2-yl)phenyl]phosphane **3b** (3 g, 0.0063 mol) and 2 N aqueous HCl (12 cm<sup>3</sup>, 0.024 mol) in THF (50 cm<sup>3</sup>) was refluxed for 15 min and then cooled to room temperature and extracted with CH<sub>2</sub>Cl<sub>2</sub> (100 cm<sup>3</sup>). The aqueous phase was neutralized with a saturated aqueous solution of sodium hydrogen carbonate and extracted with CH<sub>2</sub>Cl<sub>2</sub>. The collected

organic phases were washed with 5% sodium hydrogen carbonate aqueous solution and dried over MgSO<sub>4</sub>. After distillation of the solvents, the crude semisolid residue was purified by chromatography (CH<sub>2</sub>Cl<sub>2</sub>, neutral alumina) to afford **4b** as cream-colored crystals (1.2 g, 55% yield), mp 114 °C, lit.<sup>12</sup> 115–115.5 °C. <sup>31</sup>P NMR (CDCl<sub>3</sub>) δ: –4.9 ppm.

*Tris[4-(hydroxymethyl)phenyl]phosphane 5b.* The reduction of tris(4-formylphenyl)phosphane **4b** (0.941 g, 0.0027 mol) in dry methyl alcohol (20 cm<sup>3</sup>) by sodium borohydride (0.315 g, 0.0081 mol) under the conditions used for the reduction of **4a** afforded the triarylphosphane **5b** (0.750 g, 79% yield) as white crystals, mp 185 °C. Found: C, 71.72; H, 6.03. C<sub>21</sub>H<sub>21</sub>O<sub>3</sub>P requires C, 71.58 and H, 6.01%. <sup>31</sup>P NMR (CD<sub>3</sub>OD) δ: –4.6. <sup>1</sup>H NMR (CD<sub>3</sub>OD, 60 MHz) δ, relative to internal sodium 3-(trimethylsilyl)propionate: 7.6–7 (12H, AA'BB', ArH) and 4.5 (2H, s, CH<sub>2</sub>O).

**X-ray Crystallographic Determinations.** Colorless needles of **5a** suitable for X-ray diffraction were grown from ethyl alcohol (95%). A crystal with approximate dimensions of 0.6 × 0.4 × 0.3 mm was mounted on a glass fiber. The space group was assigned as *P*1, and the crystal system is triclinic. Intensity data were collected at 298 K on an Enraf Nonius CAD-4 diffractometer equipped with a graphite crystal incident beam monochromator using the  $\theta/2\theta$  scan mode in the index range 0° ≤ 2θ ≤ 48°, *h*<sub>max</sub> = 10, *l*<sub>max</sub> = 13. The data were collected by the CAD-4 Enraf Nonius program.<sup>13</sup> The data reduction and the structure resolution were performed by the SDP software package<sup>13</sup> by using a direct method program MULTAN.<sup>14</sup> The structure was completed by Fourier difference syntheses (10 hydrogen atoms were located in this way). Eleven hydrogen atoms were introduced at the ideal position and were included in the refinement calculations but were not themselves refined. Atomic scattering and anomalous factors were taken from *International Tables for X-Ray Crystallography*.<sup>15</sup> A sample of 2476 unique reflections was measured, and 2497 reflections with *I* ≥ 3σ(*I*) were used in structural determination. No correction for absorption or secondary extinction was made. Full matrix least-squares refinement was carried out with *w* = 1/*s*<sup>2</sup>(*I*) and converged to *R* = 0.0436, *R*<sub>w</sub> = 0.0443 for 2336 observations and 262 refined variables. Final cell constants, as well as other information pertinent to data collection and refinement, are listed in Table 1.

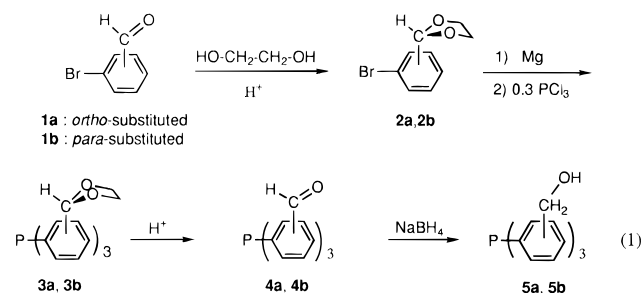
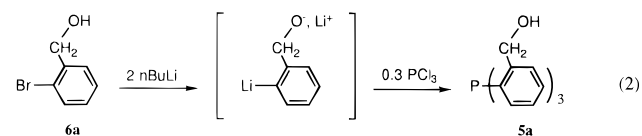
**Electrochemical Studies.** All the electrochemical experiments were performed at room temperature in acetonitrile (SDS) 0.1 M in tetra-*n*-butylammonium hexafluorophosphate (supporting electrolyte). Acetonitrile was refluxed over a mixture of KMnO<sub>4</sub> (19 g L<sup>-1</sup>) and K<sub>2</sub>CO<sub>3</sub> (18 g L<sup>-1</sup>) for 48 h, distilled, and then redistilled over P<sub>2</sub>O<sub>5</sub> (2 g L<sup>-1</sup>). The supporting electrolyte (TBAFP, Fluka, purum) was twice crystallized from a mixture of ethyl acetate and pentane (20:80) and dried at 60 °C under reduced pressure. Collidine was freshly distilled before use. Measurements were carried out on dry argon-purged solutions in three electrode cells fitted with a platinum auxiliary electrode and a Tacussel XR 110 saturated calomel electrode as reference. This reference electrode was separated from the test solution by a compartment containing the supporting electrolyte solution and closed with a porous ceramic disk. The working electrode used for both stationary and rotating disk voltammetric measurements was a Tacussel EDI 101 T platinum disk electrode (diameter, 2 mm). For coulometric and preparative electrolyses, the working electrode was a platinum foil (area, 2 or 12.5 cm<sup>2</sup>) and the used cell had separate anodic and cathodic compartments. The electrolyses were periodically interrupted to perform voltammetric monitoring at the rotating disk electrode (rotation speed, 2500 rpm).

**TABLE 1: Crystal Data, Data Collection, and Refinement Parameters**

molecular formula	C <sub>21</sub> H <sub>21</sub> O <sub>3</sub> P
formular weight	352.37
crystallization	ethanol
space group	P1(triclinic)
crystal size/mm	0.6 × 0.4 × 0.3
a/Å	10.418(4)
b/Å	10.840(7)
c/Å	8.908(6)
α	108.46(4)
β	112.21(8)
γ	63.97(0)
V/Å <sup>3</sup>	899
F(000)	186
formular unit per cell Z	2
density/g cm <sup>-1</sup>	1.302
data collection	Enraf-Nonius CAD-4 diffractometer
radiation	1MoKα
wavelength λ/Å	0.710 69
absorption coefficient μ/cm <sup>-1</sup>	1.632
monochromator	graphite
collection range 2θ/deg	1 ≤ 2θ ≤ 48
scan width	0.8 + 0.35 tan θ
h,k,l range	-10/10; -11/11; 0/13
number of reflections	
measured	2865
unique	2476
used in refinement	2497 (>3σ)
number of variables	262
R and Rw	0.0436; 0.0443
weight w	1/σ <sup>2</sup>
goodness of fit	0.636
max shift	0.01
H atoms	10 hydrogen atoms were localized on a Fourier map and refined. The 11 other hydrogen positions were calculated, not refined.

A custom-built potentiostat and data acquisition system<sup>18</sup> was used for cyclic voltammetry. Measurements at the rotating disk electrode were performed with a Tacussel PRG5 apparatus. The electrolyses were carried out at constant potential using a Tacussel PRT 100-1X potentiostat and a Tacussel IG5 electronic integrator.

**Preparation of 7a by Electrolysis of 5a.** After electrolysis at 1.1 V/SCE of tris[2-(hydroxymethyl)phenyl]phosphane in the presence of three equivalents of collidine, 90% of the solvent was evaporated. The precipitate of tetra-*n*-butylammonium hexafluorophosphate was filtered, and the solvent was then distilled to dryness. From the solid residue, the remaining electrolyte support was removed by crystallization in pentane-toluene and then by filtration. The liquid phase was neutralized with 5% acetic acid aqueous solution and dried on MgSO<sub>4</sub>. Solvents were evaporated, and the last traces of acetic acid were removed by distillation under reduced pressure (1 mmHg). 1-[2-(Hydroxymethyl)phenyl]spirobi[1*H*,3*H*-2,1-benzoxaphosphole] was isolated as a cream-colored solid (75 mg from 109 mg of electrolyzed triarylphosphane, 69% yield), mp 128 °C. Found: C, 71.76; H, 5.38. C<sub>21</sub>H<sub>19</sub>O<sub>3</sub>P requires C, 71.99; H, 5.47%. HRMS found, 350.1058. C<sub>21</sub>H<sub>19</sub>O<sub>3</sub>P requires 350.1072. IR frequencies (cm<sup>-1</sup>): 3567 (free O-H), 3450 (O-H), 1081 and 1075 (P-O), 1058 (C-O). <sup>31</sup>P NMR (CDCl<sub>3</sub>) δ: -32.0. <sup>1</sup>H NMR (CDCl<sub>3</sub>, 400.13 MHz) δ: 8.31 (2H, dd, *J*<sub>H-Hortho</sub> = 7.7 Hz, *J*<sub>HP</sub> = 10 Hz, H-6, and H-12), 7.52 (2H, tt, *J*<sub>H-Hortho</sub> = 7.7 Hz, *J*<sub>H-Hmeta</sub> = *J*<sub>HP</sub> = 1.5 Hz, H-4, and H-10), 7.45 (2H, br q, *J*<sub>H-Hortho</sub> = 7.7 Hz, *J*<sub>HP</sub> = 6 Hz, H-5, and H-11), 7.39 (1H, br dd, *J*<sub>H-Hortho</sub> = 7.6 Hz, *J*<sub>HP</sub> = 17.4 Hz, H-18), 7.33-7.23 (16 [m, 4H, H-15 (d 7.30, 1H, m, *J*<sub>H-Hortho</sub> = 7.6 Hz, *J*<sub>H-Hmeta</sub> = 1.4 Hz, *J*<sub>HP</sub> unknown), H-3 and H-9 (d 7.28, 2H, m, *J*<sub>H-Hortho</sub>

**SCHEME 2****SCHEME 3**

= 7.7 Hz, *J*<sub>HP</sub> unknown), H-16 (d 7.27, 1H, m, *J*<sub>H-Hortho</sub> = 7.6 Hz, *J*<sub>H-Hmeta</sub> = 1.5 Hz, *J*<sub>HP</sub> unknown), 7.19 (1H, tdd, *J*<sub>H-Hortho</sub> = 7.6 Hz, *J*<sub>H-Hmeta</sub> = 1.7 Hz, *J*<sub>HP</sub> = 3.3 Hz, H-17), 5.02 (2H, ABX, *J*<sub>HA-HB</sub> = 14.1 Hz, *J*<sub>HA-P</sub> = 2.9 Hz, HA of ArCH<sub>2</sub>OP), 4.90 (2H, ABX, *J*<sub>HB-HA</sub> = 14.2 Hz, *J*<sub>HB-P</sub> = 4.7 Hz, HB of ArCH<sub>2</sub>OP), 4.49 and 4.15 (2H, AB, *J*<sub>HA-HB</sub> = 11.9 Hz, ArCH<sub>2</sub>-OH), and 5.26 (s, 1H, OH). <sup>13</sup>C NMR (CDCl<sub>3</sub>, 100.6 MHz) δ: <sup>17</sup> 66.16 (d, *J*<sub>CP</sub> = 6.5 Hz, C-21), 66.59 (s, C-19 and C-20), 122.90 (d, *J*<sub>CP</sub> = 16 Hz, C-3 and C-9), 127.35 (d, *J*<sub>CP</sub> = 16 Hz, C-17), 128.19 (d, *J*<sub>CP</sub> = 13.1 Hz, C-5 and C-11), 129.17 (d, *J*<sub>CP</sub> = 160 Hz, C-1 and C-7), 129.17 (d, *J*<sub>CP</sub> = 3 Hz, C-16), 129.49 (d, *J*<sub>CP</sub> = 12 Hz, C-18), 130.93 (d, *J*<sub>CP</sub> = 14 Hz, C-15), 132.51 (d, *J*<sub>CP</sub> = 3 Hz, C-4 and C-10), 134.91 (d, *J*<sub>CP</sub> = 11 Hz, C-2 and C-6), 138.51 (d, *J*<sub>CP</sub> = 10 Hz, C-14), 140.83 (d, *J*<sub>CP</sub> = 177 Hz, C-13), and 148.05 (d, *J*<sub>CP</sub> = 26 Hz, C-2 and C-8). *m/e*: 350 (11.9%, M<sup>+</sup>), 349 (22), 332 (10.5), 321 (15.9), 320 (18.5), 319 (100), 303 (11.7), 244 (25.4), 243 (53.8), 228 (30.2), 213 (12.4), 179 (40.9), 178 (32.2), 166 (15.8), 165 (34.1), 137 (12.1), 91 (27.8), 89 (12.3), 78 (10.7), 77 (29.2), 65 (10), 63 (13.4), 57 (13.3), 55 (10.4), 51 (12.7), 47 (11.3), 43 (18.5), 39 (13.4), 31 (13.4), 29 (11.8), and 28 (14.8).

**Results and Discussion**

**Synthesis of the Triarylphosphanes.** The *ortho*-hydroxymethyl substituted triarylphosphane **5a** and the *para*-substituted isomer **5b** were prepared from the respective bromobenzaldehyde in a four-step sequence as indicated in Scheme 2. The tris(2-formylphenyl)phosphane **4a** has already been described by Schiemenz and Kaack.<sup>10</sup> Its reduction by sodium borohydride led to the tris[2-(hydroxymethyl)phenyl]phosphane **5a**, which was obtained in 43% overall yield from bromobenzaldehyde **1a**. By use of the same sequence, the tris[4-(hydroxymethyl)phenyl]phosphane **5b** was obtained in a 19% overall yield from bromobenzaldehyde **1b**. A more direct access to phosphane **5a** is a modification of the sequence used by Dahl *et al.*<sup>19</sup> in the synthesis of 3*H*-2,1-benzoxaphosphole. The lithium salt of 2-lithiobenzyl alcohol was prepared by reaction of 2-bromobenzyl alcohol with *n*-butyllithium. It was then treated with phosphorus trichloride, which led, after work-up, to **5a** in 37% yield (Scheme 3). The tris(formylphenyl)phosphanes **4a** and **4b** are relatively acid-sensitive. Indeed, deprotection of the dioxolanyl derivatives **3a** and **3b** by acid-catalyzed hydrolysis required a good control of the reaction conditions. For example, in the deprotection of **3a** catalyzed by *p*-toluenesulfonic acid in acetone, the yield of **4a** dropped from 93% to 38% when the reaction time was increased by 1 h. Moreover, when the deprotection was attempted with 2 N aqueous HCl

**TABLE 2: Selected Bond Lengths and Angles of Tris[2-(hydroxymethyl)phenyl]phosphane**

		Bond Lengths (Å)			
P–C(1)	1.836(2)	O(23)–C(20)	1.370(4)	C(2)–C(20)	1.512(5)
P–C(8)	1.846(3)	O(24)–C(21)	1.442(3)	C(9)–C(21)	1.498(3)
P–C(14)	1.836(3)	O(25)–C(22)	1.423(3)	C(15)–C(22)	1.507(2)
C(1)–C(2)	1.406(4)	C(8)–C(9)	1.398(5)	C(14)–C(15)	1.399(3)
C(1)–C(6)	1.392(4)	C(8)–C(13)	1.389(3)	C(14)–C(19)	1.397(3)
C(2)–C(3)	1.388(3)	C(9)–C(10)	1.398(4)	C(15)–C(16)	1.390(5)
C(4)–C(5)	1.373(5)	C(10)–C(11)	1.377(4)	C(16)–C(17)	1.379(4)
C(3)–C(4)	1.384(6)	C(11)–C(12)	1.373(6)	C(17)–C(18)	1.365(5)
C(5)–C(6)	1.386(3)	C(12)–C(13)	1.384(5)	C(18)–C(19)	1.386(3)
		Bond Angles (deg)			
C(1)–P–C(8)	102.4(1)	C(1)–P–C(14)	102.8(1)	C(8)–P–C(14)	101.5(1)
P–C(1)–C(2)	119.3(2)	P–C(8)–C(9)	119.5(2)	P–C(14)–C(15)	119.2(2)
P–C(1)–C(6)	121.5(2)	P–C(8)–C(13)	121.3(3)	P–C(14)–C(19)	121.8(2)
C(2)–C(1)–C(6)	118.9(2)	C(9)–C(8)–C(13)	119.1(2)	C(15)–C(14)–C(19)	119.0(2)
C(1)–C(2)–C(3)	119.2(3)	C(8)–C(9)–C(10)	118.9(2)	C(14)–C(15)–C(1)	118.9(3)
C(1)–C(6)–C(5)	121.1(3)	C(8)–C(13)–C(12)	121.1(3)	C(14)–C(19)–C(18)	120.8(3)
C(2)–C(3)–C(4)	121.0(3)	C(9)–C(10)–C(11)	120.9(3)	C(15)–C(16)–C(17)	121.4(4)
C(3)–C(4)–C(5)	120.1(3)	C(10)–C(11)–C(12)	120.2(3)	C(16)–C(17)–C(18)	119.9(4)
C(4)–C(5)–C(6)	119.8(3)	C(11)–C(12)–C(13)	119.7(3)	C(17)–C(18)–C(19)	120.0(3)
C(1)–C(2)–C(20)	121.3(2)	C(8)–C(9)–C(21)	122.1(3)	C(14)–C(15)–C(22)	122.2(3)
C(3)–C(2)–C(20)	119.5(3)	C(10)–C(9)–C(21)	118.9(3)	C(16)–C(15)–C(22)	118.9(3)
O(23)–C(20)–C(2)	111.4(2)	O(24)–C(21)–C(9)	111.2(2)	O(25)–C(22)–C(15)	110.4(3)

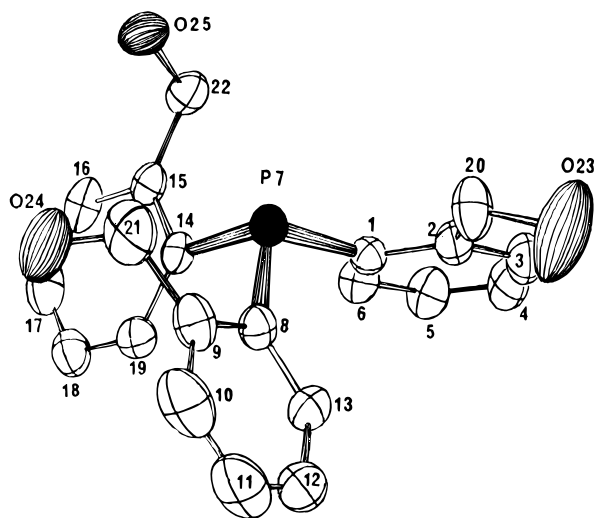
**TABLE 3: Comparative Structural Features, from X-ray Data, of Selected Triarylphosphanes and of the Tris[*o*-(hydroxymethyl)phenyl]phosphane**

Bond lengths (Å)	< C–P >	1.831	1.835	1.838	<b>1.839</b>
	a	1.393	1.400	1.413	<b>1.397</b>
	b	1.383	1.387	1.388	<b>1.389</b>
	c	1.376	1.370	1.378	<b>1.375</b>
Bond angles (°)	<θ> = < C–P–C >	102.8	102.6	109.7	<b>102.2</b>
	< C–C–P > out	116.1	118.6	114.2	<b>119.3</b>
	< C–C–P > in	124.0	122.3	127.3	<b>121.5</b>
	w	118.2	118.8	118.0	<b>119.0</b>
	x	120.8	119.9	119.4	<b>120.0</b>
	y	120.2	120.6	122.9	<b>120.5</b>
	z	120.0	120.3	117.1	<b>120.1</b>
Pyramidalisation angle (°)	α	25.52	25.69	19.24	<b>26.02</b>
	for one ring	25.0	36.7 (40.7)*	37.7 (44.1)*	<b>37.6</b>
Dihedral angles ω (°)	for the second	26.6	43.1 (45.6)*	43.3 (44.6)*	<b>39.2</b>
	for the third	59.4	49.0 (46.8)*	50.1 (44.8)*	<b>55.1</b>

\* Two estimations have been made, each of them corresponding to one of the two molecules of the unit-cell.

solution in THF for 15 min at 60 °C, a 50% yield of **4a** was obtained. In the case of the phosphane **4b**, deprotection was only performed to completion with HCl catalysis. Only a mixture of partly deprotected phosphanes was observed in the reaction with *p*-toluenesulfonic acid in acetone. This fact explains the lower overall yield in the *para*-substituted series.

**X-ray Crystallography of Phosphane 5a.** Triarylphosphanes adopt a propeller-like conformation.<sup>20</sup> The X-ray data obtained for the phosphane **5a** are reported in Tables 2 and 3, and the ORTEP<sup>21</sup> view of the molecular structure in Figure 1 shows that **5a** adopts a helicoidal geometry, with the three hydroxymethyl groups standing on the side of the phosphorus lone pair. The general structural features of **5a** are relatively close to those of the tris(2-tolyl)phosphane<sup>22</sup> or the triphenylphosphane.<sup>20</sup> The mean P–C bond length (1.839 Å) is very close to the value found for the tris(2-tolyl)phosphane (1.835 Å). However, in the case of **5a**, one of the three P–C bonds is slightly longer (1.846 and 1.836 Å for the two other

**Figure 1.** ORTEP diagram of the molecular structure of phosphane **5a**.

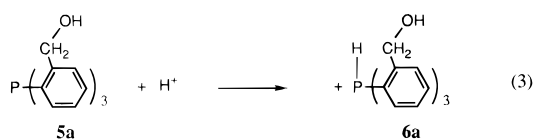
P–C bonds). The pyramidalization angle  $\alpha$  is generally governed by repulsive nonbonding interactions between the Ar groups. In the case of the tris(2,4,6-trimethylphenyl)phosphane,<sup>23</sup> an important flattening was observed ( $\alpha = 19.24^\circ$ ) compared to triphenylphosphane ( $\alpha = 25.52^\circ$ ). On the other hand, tris(2-tolyl)phosphane presented a barely different  $\alpha$  angle ( $\alpha = 25.69^\circ$ ). In phosphane **5a**, this  $\alpha$  angle was even slightly larger ( $\alpha = 26.02^\circ$ ).

For **5a**, each of the distances between the phosphorus atom and the three oxygen atoms (3.555–4.437 Å) is larger than the sum of the Van der Waals radii of phosphorus and oxygen (3.32 Å).<sup>24</sup> By contrast, because of intramolecular coordination, each of the distances between the phosphorus atom and the three nitrogen atoms (2.999–3.071 Å) in tris[2-(dimethylamino)phenyl]phosphane is smaller than the sum of the Van der Waals radii of phosphorus and nitrogen (3.4 Å).<sup>8</sup>

The X-ray study of the phosphane **5a** thus indicated that there is no specific difference in the steric effects between a hydroxymethyl or a methyl group and that the phosphorus atom does not expand its coordination number by intramolecular coordination with the three oxygen atoms.

**Electrochemical Studies.** In cyclic voltammetry at a stationary platinum electrode, the anodic oxidation of **5a** in acetonitrile

## SCHEME 4



containing 0.1M tetra-*n*-butylammonium hexafluorophosphate exhibited an anodic peak potential  $E_{pa} = 0.89$  V/SCE for a potential scan rate of  $0.1 \text{ V s}^{-1}$ . Under the same conditions, the *para*-substituted phosphane **5b** presented a higher anodic peak potential  $E_{pa} = 1.29$  V/SCE. For both phosphanes, the absence of a reverse peak, in the  $0.1\text{--}100 \text{ V s}^{-1}$  range of potential scan rates, demonstrated the low persistence of the primary product of the oxidation process. No electron paramagnetic resonance (EPR) signal could be detected when the oxidation of **5a** or **5b** was performed electrochemically within the cavity of an EPR spectrometer or by  $\gamma$ -irradiation of a freon matrix<sup>25</sup> doped with **5a** or **5b**. On the other hand, the difference in the anodic peak potential values for the two phosphanes clearly demonstrated their different electrochemical behavior although the inductive electronic effects of their substituents are similar. The phosphane **5b** could be integrated into the isosteric series of triarylphosphanes bearing one or no methyl substituent on the *ortho*-position of each phenyl ring, for which, in our previous studies, we had found a linear correlation between  $E_p$  and the  $\Sigma\sigma^+$  Hammett parameter.<sup>1,2,26</sup> However, **5a** could not be integrated in this correlation and the *ortho*-hydroxymethyl substituent appeared to have a dramatic influence on its anodic potential value.

The apparent number of electrons involved in the electron transfer for the oxidation of **5a** can be estimated by comparison to the rapid mono-electronic oxidation of the tris(2,4,6-trimethylphenyl)phosphane (TMP) under the same conditions, assuming that the diffusion coefficients for TMP and **5a** are not too different.<sup>27</sup> For potential scan rates ranging from  $0.1$  to  $10 \text{ V s}^{-1}$ , the average ratio of the anodic peak currents was

$$I_{pa}(\mathbf{5a})/I_{pa}(\text{TMP}) = 0.64$$

This value indicates that the primary step of the electrode reaction is a mono-electronic oxidation. The resultant cation radical is then quickly consumed in a chemical reaction. The small magnitude of the ratio of anodic peak currents (0.64) could imply that the phosphane **5a** diffusing to the electrode reacts partly with the chemical species generated after the primary oxidation step. In contrast, such a behavior is excluded in the case of TMP in view of the high persistence of the corresponding phosphoniumyl radical cation  $\text{TMP}^+$ .

If protons are generated during the chemical steps, as frequently observed in oxidation reactions, protonation of the phosphane **5a** would lead to the hydrophosphonium cation **6a** (Scheme 4), and this could explain the apparent decay in phosphane concentration and the low value of the ratio  $I_{pa}(\mathbf{5a})/I_{pa}(\text{TMP})$ . In order to test this hypothesis, the phosphane **5a** was oxidized in the presence of the slightly nucleophilic 2,4,6-trimethylpyridine (collidine). Under the conditions of our experiments, oxidation of collidine occurs at a potential peak of  $2.44 \text{ V/SCE}$ , thus avoiding any interference with the oxidation of **5a**. In the presence of collidine, the cyclic voltammogram of **5a** showed a greater amplitude of the oxidation peak. In this case, collidine competes with the phosphane as a proton acceptor, and the quantity of nonprotonated **5a** reaching the electrode is therefore increased.

In voltammetry at the rotating electrode, the limiting current corresponding to the oxidation wave of **5a** increased with the

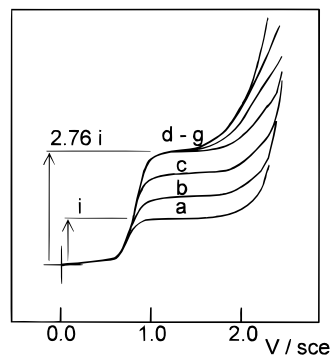


**Figure 2.** Influence of the presence of collidine on the voltammetric wave of **5a** with the following molar ratios of collidine/**5a**: (a) 0.0; (b) 0.33; (c) 0.66; (d) 1.0; (e) 1.33; (f) 1.66; (g) 2.0–3.0.

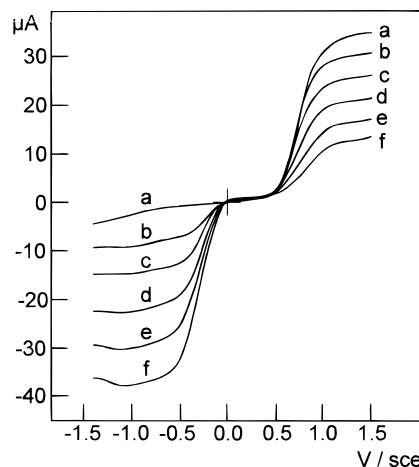


**Figure 3.** Voltammetric studies of **5a** at the rotating disk electrode in the presence of perchloric acid with the following molar ratios of acid/**5a**: (a) 0.0; (b) 0.35; (c) 0.53; (d) 0.70; (e) 0.88; (f) 1.06.

concentration of collidine up to a constant value reached for a molar ratio [collidine]/**5a** of 3 (Figure 2). At this point, the measured current was 2.76 times the current obtained in the absence of collidine.

Under nitrogen atmosphere, in acetonitrile containing  $0.1 \text{ M}$  TBAFP, a preparative electrolysis was conducted, without collidine, at a potential corresponding to the limiting current of the **5a** anodic wave. The progress of the electrolysis was monitored by voltammetry at the rotating electrode. A regular decrease of the oxidation wave of **5a** at  $E_{1/2} = +0.75 \text{ V/SCE}$  was observed together with the appearance and increase of a reduction wave at  $E_{1/2} = -0.25 \text{ V/SCE}$ . Integration of the electrolysis current value gave a total apparent number of 1.1 electrons exchanged per molecule.

Attribution of the cathodic wave to the reduction of **6a** (Scheme 4), which is generated during the electrolysis, is supported by the results of voltammetric measurements on **5a** in acidic medium (Figure 3). When a dilute solution of  $\text{HClO}_4$  in acetonitrile was added to the voltammetric solution of **5a**, a wave appeared at  $E_{1/2} = -0.25 \text{ V/SCE}$ , the limiting current of which varied linearly with the amount of  $\text{HClO}_4$ . A corresponding decrease of the intensity of the oxidation wave of **5a** was also observed.

When a preparative electrolysis was performed on **5a** in the presence of collidine, with a molar ratio [collidine]/**5a** of 3 (Figure 4), the oxidation wave of **5a** decreased during the course of electrolysis. A plot of the voltammetric current  $I$  toward the electric-charge-consumed  $Q$  is shown on Figure 5. Extrapolation at  $I = 0$  for the value of the voltammetric current gave a total apparent number of 1.8 exchanged electrons per molecule.

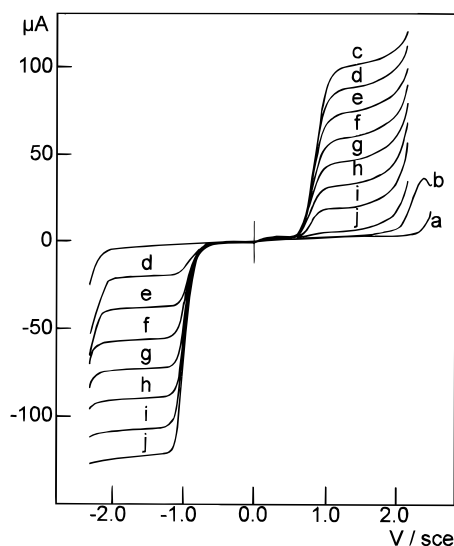


**Figure 4.** Selected voltammetric curves recorded during the progress of the electrolysis of **5a** (0.338 mmol) in the presence of an excess of collidine (molar ratio 3:1): (a) residual current; (b) residual current with added collidine; (c)  $Q = 0$  C; (d)  $Q = 8.1$  C; (e)  $Q = 16.2$  C; (f)  $Q = 24.6$ ; (g)  $Q = 32.4$  C; (h)  $Q = 40.5$  C; (i)  $Q = 48.6$  C; (j)  $Q = 56.7$  C.

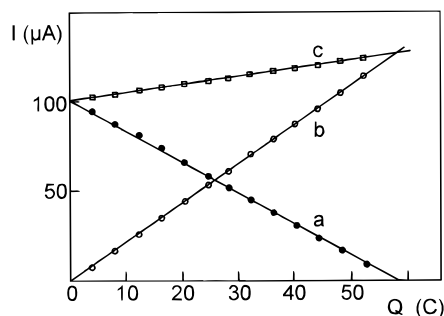
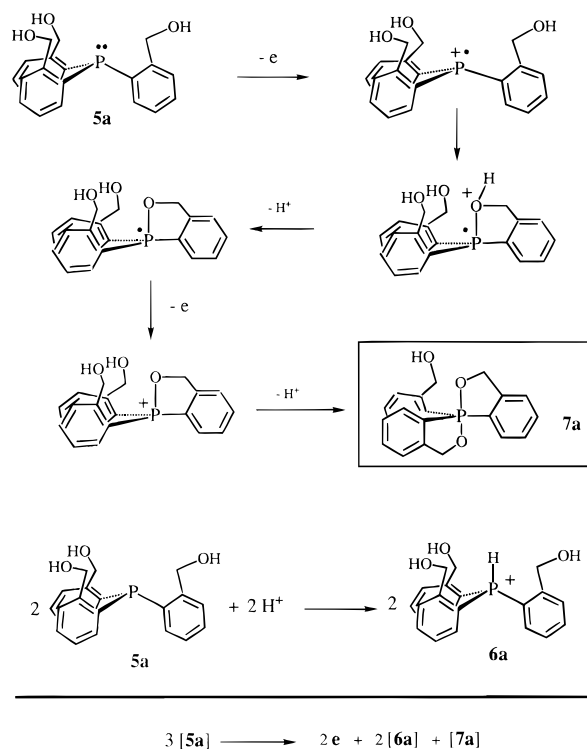


**Figure 5.** Evolution of the voltammetric currents during the electrolysis of **5a** in the presence of collidine (3:1): (a) limiting current of **5a**; (b) limiting current of collidinium (absolute value); (c) sum.

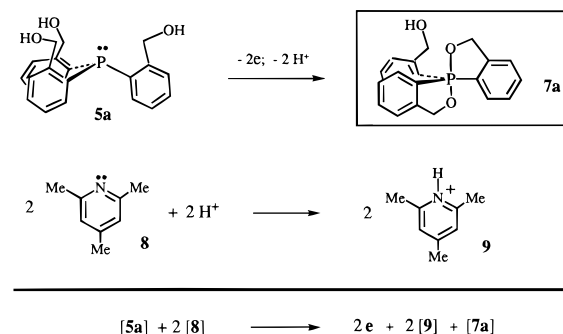
A cathodic wave appeared at  $E_{1/2} = -0.95$  V/SCE, attributed to the reduction wave of the collidinium cation generated during the electrolysis by protonation of the collidine. There was no evidence for the presence of **6a** since no wave near  $-0.25$  V/SCE was present.

The electrochemical behavior of **5a** in the absence of collidine or in the presence of a sufficient amount of collidine can be explained by the mechanisms described in Schemes 5 and 6. In both cases, the first step is the monoelectronic oxidation of **5a** leading to the cation radical **5a**<sup>•+</sup>. Intramolecular reaction between the positively charged phosphorus center and the oxygen of the *ortho*-hydroxymethyl substituent of one aromatic ligand creates a strong P–O bond together with the release of a proton. The proton is trapped either by the nonoxidized **5a** diffusing to the electrode (Scheme 5) or by collidine (Scheme 6), leading to the corresponding phosphonium or ammonium cation. The loss of the proton generates a cyclic phosphoranyl radical, which is probably easily oxidized, contributes to the electron transfer at the actual working potential (ECE mechanism). Alternatively, the cyclic phosphoranyl radical could react with the phosphoniumyl cation radical in a homogeneous electron transfer reaction as presented in Scheme 7 (DISP mechanism).<sup>28</sup> The ensuing cationic species undergoes a second intramolecular attack, leading to the stable 1-[2-(hydroxymethyl)phenyl]spirobi-[1H,3H-2,1-benzoxaphosphole] **7a** with the release of a second

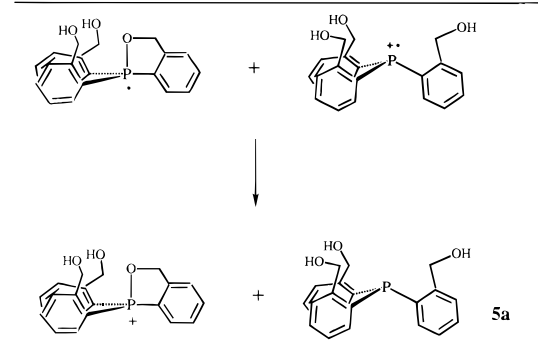
### SCHEME 5



### SCHEME 6



### SCHEME 7



proton. In both cases, either an ECE (Scheme 5 and 6) or a DISP mechanism, the same global reaction balance is obtained.

In the absence of collidine, two electrons are transferred for the consumption of three molecules of **5a** and the formation of

**TABLE 4: Calculation of Ratio between Oxidized Amount of **5a** and the Amount of Collidinium ( $\Delta C_{\text{col}}/\Delta C_{5a}$ ) Formed during the Electrolysis of **5a****

$\Delta Q^a$ (C)	$I_{\text{la}}^b$ ( $\mu\text{A}$ )	$I_{\text{ra}}^c$ ( $\mu\text{A}$ )	$C_{5a}^d$ (mol L $^{-1}$ )	$C_{\text{col}}^e$ (mol L $^{-1}$ )	$\Delta C_{\text{col}}/\Delta C_{5a}$
0.00	101.0	0.0	$1.47 \times 10^{-3}$	0.00	
4.05	94.5	7.5	$1.37 \times 10^{-3}$	$1.72 \times 10^{-4}$	1.72
8.10	88.0	16.5	$1.28 \times 10^{-3}$	$3.78 \times 10^{-4}$	1.99
12.15	81.0	25.5	$1.18 \times 10^{-3}$	$5.84 \times 10^{-4}$	2.01
16.20	73.5	34.5	$1.07 \times 10^{-3}$	$7.90 \times 10^{-4}$	1.98
20.25	66.0	44.0	$9.60 \times 10^{-4}$	$1.01 \times 10^{-3}$	1.98
24.60	58.5	53.5	$8.51 \times 10^{-4}$	$1.22 \times 10^{-3}$	1.97
28.35	52.0	61.5	$7.57 \times 10^{-4}$	$1.41 \times 10^{-3}$	1.98
32.40	45.0	71.0	$6.55 \times 10^{-4}$	$1.63 \times 10^{-3}$	2.00
36.45	38.0	80.0	$5.53 \times 10^{-4}$	$1.83 \times 10^{-3}$	2.00
40.50	31.0	88.5	$4.51 \times 10^{-4}$	$2.03 \times 10^{-3}$	1.99
44.55	24.5	97.0	$3.56 \times 10^{-4}$	$2.22 \times 10^{-3}$	1.99
48.60	17.5	106.5	$2.55 \times 10^{-4}$	$2.44 \times 10^{-3}$	2.01
52.65	10.0	116.0	$1.46 \times 10^{-4}$	$2.66 \times 10^{-3}$	2.01

<sup>a</sup> Amount of charge. <sup>b</sup> Limiting current of oxidation of **5a**. <sup>c</sup> Limiting current of reduction of collidinium. <sup>d</sup> Concentration of **5a**. <sup>e</sup> Concentration of collidinium.

one molecule of **7a** and two molecules of **6a**. This is in clear agreement with the peak current ratio [ $I_{\text{pa}}(\mathbf{5a})/I_{\text{pa}}(\text{TMP}) = 0.64$ ] and with the appearance, during the electrolysis, of the reduction wave attributed to **6a**. However, this mechanism cannot explain the coulometric result ( $n = 1.1$ ) obtained for the total number of electrons exchanged. This discrepancy could be imputed to the importance of the concentration changes during coulometry and to the reversibility of the phosphane protonation.

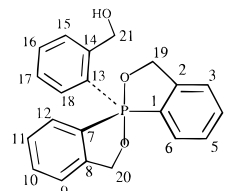
It is worth considering that the phosphonium cation **6a** generated during the electrolysis is positively charged at the phosphorus center and that an intramolecular reaction with the side chain oxygen atoms could occur. If such a reaction would be likely to occur at an appreciable rate, the phosphonium cation prepared by addition of HClO<sub>4</sub> in a solution of **5a** should not be stable. But this is not evidenced by the voltammetric experiments, which showed constant limiting currents under such conditions.

On the other hand, in the presence of collidine the second mechanism described in Scheme 6 is in relatively good agreement with the electrochemical results obtained. For each molecule of **5a**, two electrons must be exchanged, and the experimental value is  $n = 1.80$ . The presence of the collidinium cation among the products of electrolysis is supported by the appearance of the reduction wave at  $E_{1/2} = -0.95$  V/SCE.

Voltammetric studies on authentic samples of collidinium *p*-toluenesulfonate and collidinium chloride indicated that, in the concentration range from  $5 \times 10^{-4}$  to  $2.5 \times 10^{-3}$  M, the limiting current ( $i_l$ ) is proportional to the concentration ( $C$ ) of collidinium [for collidinium chloride  $C/i_l = 2.29 \times 10^{-5}$  mol L $^{-1}$  mA $^{-1}$  and for collidinium *p*-toluenesulfonate  $C/i_l = 2.24 \times 10^{-5}$  mol L $^{-1}$  mA $^{-1}$  under the same experimental conditions as those of electrolysis monitoring (2 mm rotating disk electrode diameter, 2500 rpm)].

The mean value of the proportionality coefficient was used to determine the quantity of collidinium cations generated during the electrolysis. For each voltammetric monitoring curve, the concentration of the remaining **5a** (assuming proportionality between limiting current and concentration) and that of the collidinium salt were computed (Table 4). As predicted according to Scheme 6, the ratio between the quantity of generated collidinium and the quantity of consumed **5a** is very close to 2.

Workup of the electrolysis solution mixture afforded the spirobi[benzoxaphosphole] **7a** (Figure 6), which was isolated in a 69% yield.

**Figure 6.** Structure and numbering of the spirobi[benzoxaphosphole] **7a**.

All these results led us to conclude that the electrochemical behavior of **5a** in acetonitrile and in the presence of an excess of an organic base is correctly described by Scheme 6. When no base is added, Scheme 5 may be used to explain the behavior of **5a**, although some mechanistic complications are likely to occur. Since the phosphane is a less efficient base than collidine and, moreover, its concentration decreases during the electrolysis, then the reversible deprotonation of the phosphonium can increase the disponibility of **5a**. The electrochemical behavior of **5a** may be called a self-deprotonation mechanism, which is quite similar to a self-protonation mechanism. A very interesting and detailed study on the kinetics of the self-protonation reaction in organic electrochemical processes has been reported by Amatore *et al.*<sup>29</sup>

## Conclusion

According to the X-ray diffraction results, the tris[2-(hydroxymethyl)phenyl]phosphane **5a** does not exhibit any oxygen–P<sup>III</sup> interaction although the three oxygen atoms are on the same side as the phosphorus electron lone pair. In the presence of an efficient proton trap such as collidine, electrochemical experiments led us to conclude that the low value of the anodic peak observed for **5a** was the consequence of the occurrence of an ECE (or DISP) global process involving the transfer of two electrons and the release of two protons. After the first electron transfer, the geometry of formed **5a**<sup>+</sup> is appropriate to favor its fast decay through the intramolecular formation of a P–O bond, leading to an intermediate phosphoranyl radical. Subsequent oxidation of this phosphoranyl followed by a second cyclization step finally gave rise to the 1-[2-(hydroxymethyl)phenyl]spirobi[1*H*,3*H*-2,1-benzoxaphosphole] **7a**, which was isolated in 69% yield by controlled potential preparative electrolysis. In the absence of collidine, a fraction of **5a** was protonated and became electrochemically inactive at the oxidation potential used in the experiments.

The anodic behavior and the ESR characterization at 77 K in Freon matrices of the cation radicals of tris[2-(methoxymethyl)phenyl]phosphane, tris[2-((methylthio)methyl)phenyl]phosphane and tris[2-((dimethylamino)methyl)phenyl]phosphane will be reported in a forthcoming paper.

## References and Notes

- (1) Culcasi, M.; Berchadsky, Y.; Gronchi, G.; Tordo, P. *J. Org. Chem.* **1991**, *56*, 3536.
- (2) Palau, C.; Berchadsky, Y.; Chaliier, F.; Finet, J.-P.; Gronchi, G.; Tordo, P. *J. Chem. Phys.* **1995**, *99*, 158.
- (3) Tomaschewski, G. *J. Prakt. Chem.* **1966**, *33*, 1339.
- (4) Redouane, N.; Vila, F.; Chaliier, F.; Gronchi, G.; Tordo, P. *Phosphorus, Sulfur Silicon Relat. Elem.* **1993**, *77*, 101.
- (5) Gilheany, D. G. *Chem. Rev.* **1994**, *94*, 168.
- (6) McEwen, W. E.; Shiau, W.; Yeh, Y. I.; Schulz, D. N.; Pagilagan, R. U.; Levy, J. B.; Symmes, C., Jr.; Nelson, G. O.; Granth, I. *J. Am. Chem. Soc.* **1975**, *97*, 1787.
- (7) Cairns, S. M.; McEwen, W. E. *Heteroat. Chem.* **1990**, *1*, 9.
- (8) Chuit, C.; Corriu, R. J. P.; Montforte, P.; Reyé, C.; Declercq, J.-P.; Dubourg, A. *Angew. Chem., Int. Ed. Engl.* **1993**, *32*, 1430.
- (9) Miller, G. R.; Yankowsky, A. W.; Grim, S. O. *J. Chem. Phys.* **1969**, *51*, 3185.
- (10) Schiemenz, G. P.; Kaack, H. *Liebigs Ann. Chem.* **1973**, 1480.

- (11) Hoffmann, A. K.; Thomas, W. M. *J. Am. Chem. Soc.* **1959**, *81*, 580.
- (12) Bartlett, P. A.; Bauer, B.; Singer, S. J. *J. Am. Chem. Soc.* **1978**, *100*, 5085.
- (13) Frenz, B. A. In *The Enraf Nonius CAD-4 SDP-A Real Time System for Concurrent X-ray Data Collection and Crystal Structure Solution in Computing in Crystallography*; Schenk, H., Olthof-Hasekamp, R., van Koningsveld, H., Bassi, G. C., Eds.; Delft University Press: Delft, 1978; pp 64.
- (14) Main, P.; Fiske, S. J.; Hull, S. E.; Lessinger, L.; Germain, G.; Declercq, J. P.; Woolfson, M. N. In *MULTAN 80, A System of Computer Programs for the Automatic Solution of Crystal Structure from X-ray Diffraction Data*; Universities of York, England and Louvain: Belgium, 1980.
- (15) Ibers, J., Hamilton, W. C., Eds. *International Tables for X-Ray Crystallography*; Kynoch Press: Birmingham (present distributor, Kluwer Academic Publishers: Dordrecht), 1974; Vol. IV.
- (16) The chemical shift and proton-proton coupling constants were determined by COSY HH and <sup>1</sup>H NMR with phosphorus coupling by using reverse probe.
- (17) The chemical shifts were assigned by HMQC spectrum elucidation.
- (18) Berchadsky, Y.; Gronchi, G. Système d'acquisition BYGG-AEL. *Catalogue de l'Agence Nationale du Logiciel (France)*; Société Française de Chimie: Paris, November 1991.
- (19) Dahl, B. M.; Dahl, O.; Trippet, S. *J. Chem. Soc., Perkin Trans. 1* **1981**, 2239.
- (20) Dunne, B. J.; Orpen, A. G. *Acta Crystallogr., Sect. C* **1991**, *45*, 345.
- (21) Johnson, C. K. ORTEP Report ORNL-3794; Oak Ridge National Laboratory: Tennessee, 1965.
- (22) Cameroun, S. T.; Dahlèn, B. *J. Chem. Soc., Perkin Trans. 2* **1975**, 1737.
- (23) Blount, J. F.; Maryanoff, C. A.; Mislow, K. *Tetrahedron Lett.* **1975**, 913.
- (24) Bondi, A. *J. Phys. Chem.* **1964**, *68*, 441.
- (25) Eastland, G. W.; Symons, M. C. R. *J. Chem. Soc., Perkin Trans. 2* **1977**, 833.
- (26) Culcasi, M.; Gronchi, G.; Tordo, P. *Phosphorus Sulfur Relat. Elem.* **1987**, *30*, 511.
- (27) This method was also used by Romakhin, A. S.; Nikitin, E. V.; Parakin, O. V.; Ygnat'ev, Yu. A.; Mironov, B. S.; Kargin, Yu. M. *Zh. Obshch. Khim.* **1986**, *56*, 259.
- (28) Savéant, J. M. *Acc. Chem. Res.* **1993**, *26*, 455. Andrieux, C. P.; Savéant, J. M. In *Electrochemical Reaction. Investigation of Rates and Mechanism of Reactions*; Bernasconi, C. F., Ed.; Techniques of Chemistry, Vol. 6 (2); John Wiley & Sons: New York, 1986; Chapter 7, p 305. Evans, D. H. *Chem. Rev.* **1990**, *90*, 739, and references therein.
- (29) Amatore, C.; Capobianco, G.; Farnia, G.; Sandonà, G.; Savéant, J. M.; Severin, G.; Vianello, E. *J. Am. Chem. Soc.* **1985**, *107*, 1815.

JP952854P